SWATLitho: A hydrogeochemical model to estimate daily geochemical loads at the catchment scale

Juan Luis Lechuga-Crespo, Sabine Sauvage, Estilita Ruiz-Romera, Chris George, J.M. Sánchez-Pérez

SWATLitho: a hydrogeochemical model to estimate daily geochemical loads at the catchment scale.

Juan Luis Lechuga-Crespo[1,2*], Sabine Sauvage[2], Estilita Ruiz-Romera[1], Chris George[3], José Miguel Sánchez-Pérez[2*]

[1] Department of Chemical and Environmental Engineering, University of the Basque Country, Plaza Ingeniero Torres Quevedo 1, Bilbao 48013, Basque Country, Spain

[2] Laboratoire Ecologie fonctionnelle et Environnement, Université de Toulouse, CNRS, INP Toulouse, UPS, Campus ENSAT, Avenue de l'Agrobiopole, 31326 Castanet Tolosan CEDEX, France

[3] Formerly United Nations University International Institute for Software Technology, Macao

*Corresponding author: Juan Luis Lechuga-Crespo (juanluis.lechuga@ehu.eus) and José-Miguel Sanchez-pérez (Jose.sanchez@univ-tlse3.fr)

Highlights

- A lithological layer coupled to SWAT Hydrological Response Units has been introduced.
- A simple model has been implemented to assess daily cation and anion fluxes.
- Daily geochemical loads have been estimated using SWAT water balance.

Abstract

The increase in water salinisation in catchments has led to increased concern in assessing major ion loadings in freshwater environments. In this study, we couple a globally fitted model on chemical weathering to the Soil and Water Assessment Tool (SWAT) for the estimation of daily geochemical loadings at the catchment scale, "SWATLitho". The enhancements include *i)* a modification on the discretisation of the catchment area by integrating a layer describing lithology (QSWATLitho), and *ii)* the development of an extra module to compute the ionic loads derived from the chemical weathering of rocks. The model is sensitive to input data resolution, yielding the best results when including local data. Larger spatial and temporal discrepancies are found in one tributary, associated with point sources impacting the loadings; while these discrepancies are lower at headwater subbasins. Results suggest that, despite of these discrepancies, the average simulation of the daily ionic loadings is reasonable.

Keywords

Model coupling; Geochemical loadings; Chemical weathering; Downscaling

1 Introduction

Chemical quality assessment of river waters is crucial for understanding and assessing the potential impacts of threats to biodiversity, drinking water safety, and crop yields (Cañedo-Argüelles et al., 2018, Kaushal et al., 2017). One of these threats is the rise in major ion concentration, i.e. salinisation (Meybeck and Helmer, 1989), which, despite having a relevant role in efficient ecosystem management (Cañedo-Argüelles et al., 2018), has received little attention in the past. Traditionally, two approaches tackling freshwater chemical assessments exist: the analysis of water samples framed within a monitoring program (e.g. Martínez-Santos et al., 2015), and the use of hydrogeochemical models to simulate the study area and possible scenarios (e.g. M'Nassri et al., 2019). Water sampling is a common practice in many places, yielding real valuable data, but spatially and temporally homogeneous information is obtained through modelling. The integration of these two approaches complements the assessment of chemical threats.

Models may be based on physical laws or data-regression equations for representing the system object of the study, being classified as mechanistic or empirical, respectively. Nowadays, there exists a number of mechanistic hydrogeochemical models, such as PHREEQC (Version 3 in Parkhust and Appelo, 2013), MINTEQA2 (Allison et al., 1991), or WITCH (Goddéris et al., 2006), but their applicability is commonly limited to areas where extensive necessary data (mineral abundance, the chemical profile of soil water, initial boundary condition, etc.) is available as input. In other cases, simplifications or assumptions are needed in order to apply this kind of model, increasing the model's prediction uncertainty. A different solution is to develop simpler models to replace these complex configurations (Schoups et al., 2006).

As an alternative to mechanistic models, several empirical models focusing on single-processes have been built, such as the Global Erosion Model for CO_2 (GEM-CO_2, Amiotte-Suchet and Probst, 1995), the Chemical Weathering Rate model (CWR, Hartmann et al., 2014) and Ionic fluxes derived from Chemical Weathering of Rocks model (ICWR, Lechuga-Crespo et al., 2020a), which have yielded a static output over worldwide scale assessments, i.e. the annual average result, regarding chemical weathering rates and associated products (atmospheric CO_2 consumption, P-release, ionic loadings to rivers, etc.). To date and to the best of the authors' knowledge, none of them have been tested on a local scale and under a dynamic approach, while management decisions are usually taken at a catchment scale and need the temporal evolution within a year.

In the present study, an empirically-based model has been coupled to a physically-based hydrological model to compute daily geochemical loadings from the chemical weathering of rocks. The SWAT model has long been used to quantify the loads and concentrations of matter and nutrients from land to the catchment's outlet (Arnold et al., 2012, Fu et al., 2019), as well as its evolution at different time scales. However, it is not possible to estimate the geochemical loadings with this model, as there is no subroutine or module implemented with this purpose. In this sense, the ICWR model (Lechuga-Crespo et al., 2020a) has been applied to the global scale. It has yielded the first map on average annual ionic fluxes, derived from the

chemical weathering of rocks to rivers. Nevertheless, its ability to simulate the dynamics of chemical weathering derived ionic loads and its performance on local catchments have not been tested yet.

In this sense, the coupling of the SWAT and ICWR models poses an opportunity to evaluate spatially-explicit geochemical fluxes, since a basin's hydrology in SWAT is described using the Hydrological Response Unit's (HRU) semi-distributed approach . Consequently, ionic loadings from chemical weathering may be assessed and, if the atmospheric contribution is known, this tool may work with observed data to estimate how much anthropogenic saline effluent found in a catchment. It is important to note that a similar approach has been recently published by Bailey et al. (2019), where they present the coupling of a mechanistic model for major ion chemical partitioning within the SWAT hydrological code. Such mechanistic methodology presents the same constraints in application as the other mechanistic approaches: the availability of input data and the establishment of boundary conditions for simulation.

The objective of this study is to downscale the ICWR model spatially and temporally as well as explore the performance in a case study where a geochemistry monitoring program has been taken. This case is exploratory, and the model objectives are to simulate the daily geochemical loads of major ions and their spatial distribution. Given the modelling framework and the constraints of both models, the processes to be simulated are chemical weathering of rocks, mass transport, and routing from catchment subbasins to the outlet. The model's spatial definition is conditioned by the HRU delimitation of the modified model (which is explained in Section 2.2), while the simulation's time-step is daily. A chemical equilibrium is assumed between rock and water at the temporal scale of simulation. Then, loadings are expected to be dependent on the discharge distribution among groundwater, lateral, and surface fluxes; the lithological groups in the underlying rock; and the soil types.

2 Methods

2.1 Overview of the SWAT and the ICWR models

The Ionic fluxes derived from Chemical Weathering of Rocks (ICWR, Lechuga-Crespo et al., 2020a) model is empirically based and its parameters have been fitted at a global scale for the estimation of spatially explicit fluxes of chemical weathering of rocks F, measured in $mol \cdot m^{-2} \cdot y^{-1}$ for each major ion Ca^{2+}, Mg^{2+}, Na^{+}, K^{+}, SO_4^{2-}, Cl^{-}, and alkalinity (commonly associated with HCO_3^{-}). The model configuration is based on the multivariable regression shown in Equation 1. The input data needed for this model includes the specific discharge q_{ann} measured in mm, the lithological composition of the rocks L_i expressed as the percentage of the catchment area covered by a lithological group, the soil covering the bedrock layer for the estimation of the soil shielding effect factor f_{sx}, which is different for each ion x, and the parameter of the equation C_{xi}, representing the water concentration on every ion. Further explanation of the development, calibration, and limitations of the model can be seen in Lechuga-Crespo et al. (2020a). The output of this model is an annual average specific flux of major ion loads originating from the chemical weathering of rocks to rivers, which,

together with atmospheric deposition and anthropogenic inputs, is the main reservoir of saline exports of a basin.

$$F_x = q_{ann} \cdot f_{s_x} \cdot \sum L_i \cdot C_{x_i} \qquad \textbf{Equation 1}$$

The SWAT is a physically based and semi-distributed model developed to assess water, sediments, and nutrients in agronomic catchments at yearly, monthly, daily, and sub-daily time steps (Arnold et al., 1998). Water, matter, and nutrient balances are simulated in homogeneous spatial units, HRUs, a combination of unique slope, land use, and soil type areas, which are then aggregated to the subbasin scale and routed through tributaries and channels towards the outlet of the catchment. The HRUs, together with the weather data (at least precipitation and temperature time series), provide the input data for the simulation. A more detailed description of the model is available in the SWAT2012 theoretical handbook (Neitsch et al., 2011).

2.2 Coupling the ICWR model to SWAT

The approach to spatially discretising the catchment area in the SWAT model has been modified to include a fourth layer in the definition of the HRUs: the lithological groups. This modification has been performed in the QGIS geographic information system plugin used to set up the model, QSWAT (Dile et al., 2016); the modified version is hereby called QSWATLitho. The SWAT code has not been modified to maintain the possibility of using external software, such as SWAT CUP (Abbaspour et al., 2007), for autocalibration. Instead, an extra module (SWATLitho.py) has been written to read the QSWATLitho and SWAT outputs and compute the geochemical fluxes and loads. The workflow of the model's configuration is shown in Figure 1.

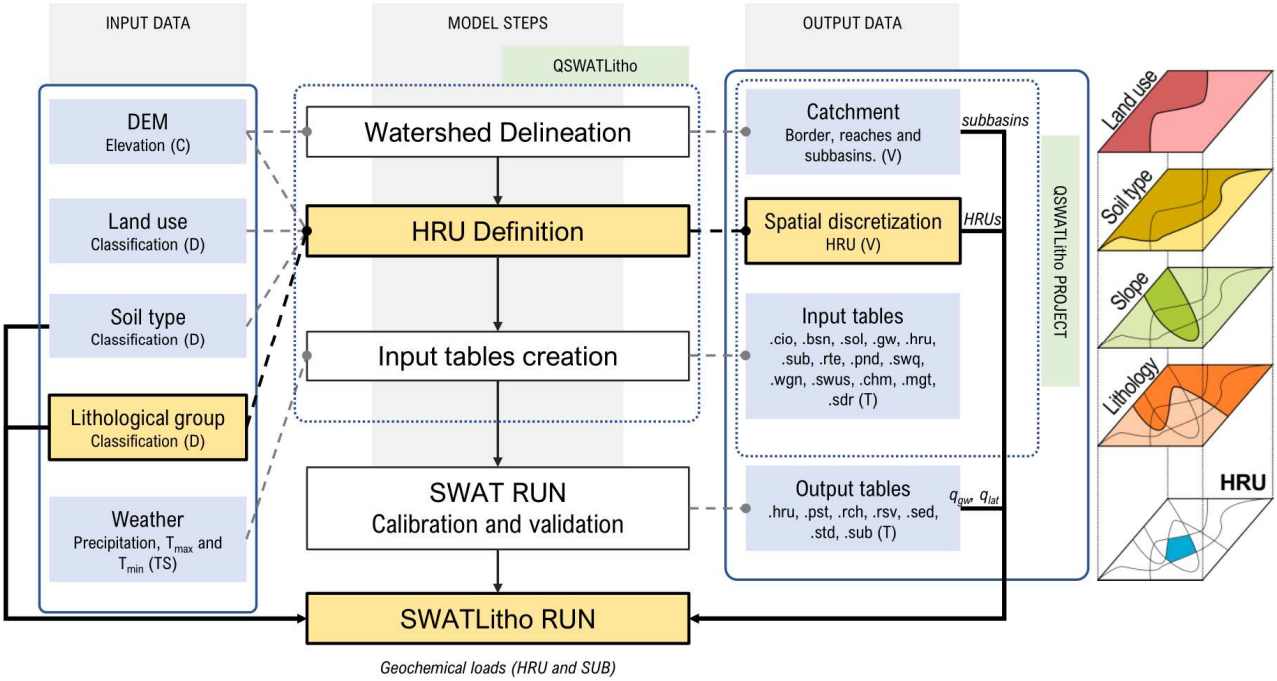

Figure 1. Workflow summary of the ICWR model implemented on the modified QSWAT. The modifications accomplished in the input data, model steps, and output data are highlighted in yellow (the reader is referred to

the online version for the colour appreciation). Bold arrows indicate the input data for the SWATLitho module for the estimation of the geochemical loads. On the right side, there is a conceptual representation of the new delimitation of the HRUs.

2.2.1 QSWATLitho

Traditionally, a QSWAT model setup consists of three main phases: the delineation of the watershed and subbasins, the delimitation of the HRUs, and the write of the input tables for SWAT modelling. For the QSWATLitho implementation, the second step has been modified by changing the *hrus.py*, *DBUtils.py*, and *QSWATUtils.py* files in the original plugin, causing the inclusion of a new layer to the delimitation of the HRUs. Now, every HRU contains a unique combination of slope, land use, soil type, and lithological group, and the water balance is defined for each one of them. The first consequence of this change is an increased number of HRUs when setting up a project, causing a finer definition on the spatial distribution of the model outputs and an increase in the time used for the SWAT simulation. The QSWATLitho may be found and downloaded at https://swat.tamu.edu/software/swat-litho/.

2.2.2 ICWR module - SWATLitho

Once a QSWATLitho project has been set up, the calibration of the hydrology is needed, since this is the main dynamic input data for the ICWR model. Because the chemical weathering process occurs mainly in the vadose zone of the water cycle, the main water fluxes to be considered are groundwater (q_{gw}) and lateral flows (q_{lf}). The ICWR model has been adapted to include them (q_{lf}+q_{gw}) instead of the total average specific discharge (q_{ann}), which would also include runoff. Here, the runoff is considered as the main driver for the dilution of the total load rather than including it in the calculation of the daily geochemical loads. A new module has been created so that the user can use the SWAT results, in combination with the QSWATLitho tables, to obtain geochemical loadings' daily time series. The module consists of six main steps that are integrated into two loops. For each HRU, data like area, lithological group, and soil type is extracted from the *hrus_lithology.csv* file (a modified version of the *hrus* file in the *Project.mdb*) and, if necessary, used to set the soil shielding effect, f_{sx} (cf. Lechuga-Crespo et al., 2020a). Then, the *output.hru* file is read to obtain the specific discharge in the lateral and groundwater fluxes to the river. With this information, together with the globally fitted parameters, the geochemical loads are calculated for each time step of the simulation and each HRU. This process generates a table with the loads of each HRU to the river stream for each time step. Then, all of the loadings are summarised at the subbasin scale in each time step and saved as output. The geochemical loadings are routed by adding the upstream loadings (if such exists) to the contribution of each subbasin draining area. A workflow summary is shown in Figure 2, and the modified version of the ICWR regression (Equation 1) is shown in Equation 2, where L_x represents the loading of ion x in each HRU (in $Mg \cdot d^{-1}$), A is the area of the catchment in m^2, q_{GW+LT} accounts for lateral and groundwater-specific discharge (mm), respectively, f_{sx} represents the soil shielding effect (dimensionless), and $C_{Lit,x}$ is the globally fitted

parameter for each lithological unit and ion (mol·L^{-1}). Note that units are adjusted depending on the ion that is being considered and that this modification considers each HRU to be a monolithic unit to the river stream.

$$L_x = A_{HRU} \cdot (q_{GW+LT}) \cdot f_{s_x} \cdot C_{Lit_x} \quad \text{Equation 2}$$

The lithological groups used in the ICWR model development study are kept unaltered in the present development: evaporites (ev), metamorphics (mt), plutonic acid (pa), plutonic basic (pb), plutonic intermediate (pi), pyroclastics (py), sediment carbonates (sc), sediment mixed (sm), sediment siliciclastic (ss), sediment unconsolidated (su), volcanic acid (va), volcanic basic (vb), volcanic intermediate (vi), water bodies (wb), ice and glaciers (ig), and no data (nd), according to the description presented in Hartmann and Moosdorf (2012) and Dürr et al. (2005).

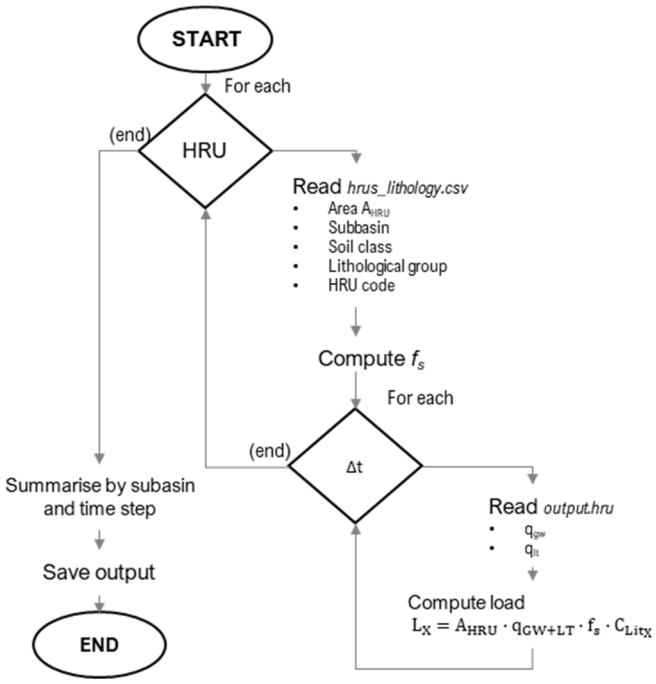

Figure 2. Workflow of the algorithm used to estimate the chemical weathering loadings from the outputs of the QSWATLitho project calibrated for discharge. Ellipses indicate the start and end of the algorithm. The diamonds represent the loops: one for each HRU in the project and another for each time step (Δt) simulated (year, month, day). The arrows indicate the action sequence.

2.3 Case study: Deba River catchment

A case study is set up to explore the model's application. The validation comprises three steps: first, the annual comparison of the results to evaluate the model's sensitivity and select the input data among different combinations; second, the analysis of geochemical loadings in all subbasins derived from the QSWATLitho + SWATLitho combination (spatial downscaling); and last, the comparison of the daily representation in three gauging stations (temporal downscaling). The case study selected for this purpose is the Deba River catchment (Figure 3), on which numerous studies related to urban and industrial pollution on its sediments and waters have been conducted (Martínez-Santos et al., 2015; García-García et al., 2019; Unda-Calvo et al., 2019; Lechuga-Crespo et al., 2020b). There are eleven sampling locations along its main channel and tributaries,

where a monitoring campaign was established between April 2014 and January 2017. Samples were taken in a monthly or bi-monthly time step. In addition, there are three gauging stations measuring, among other variables, discharge and electrical conductivity every 10 minutes.

2.3.1 Study area

The Deba River Basin has a complete drainage area of 538 km^2 and 60 km of main stream, a maximum slope of 40%, and an elevation varying from 0 at sea level to 1,320 m in Botreatiz (the highest mountain), which is located in the northern part of Spain, in the Gipuzkoa Province in the Basque Country (Figure 3). Regarding its hydrometeorology, there is a strong variation between humid and dry years, as well as a strong seasonal variability: about 30% of the total annual water volume is exported in December and January, and in dry summers, the specific discharge can reach 0.6 mm. The average annual precipitation is estimated to be 1,613 mm, while the mean temperature is 12.7ºC, leading to the highest potential evapotranspiration (ETP) of the surrounding catchments at 871 mm. In terms of the occupation of this catchment, there is a strong presence of industries, with a population of 135 000 inhabitants grouped into four important villages (Arrasate, Oñati, Bergara, Eibar, and Deba); 37% of the area is occupied by *Pinus spp*; 27% is covered by autochthonous forest, and 11% is given to farmlands and pastures. This catchment is commonly located over evaporitic rocks (gypsum and anhydrite deposits) included in detrital rocks, which, according to the classification proposed by Hartmann and Moosdorf (2012) and Dürr et al. (2005), correspond to a mix of siliciclastic, carbonate and mixed sediments, together with other lithological groups. A detailed description of the geology of the zone is addressed in Ábalos et al. (2008) and Iribar and Ábalos (2011). Historically, this catchment has suffered a strong urban and industrial pressure (Gipuzkoa Council, accessed on October 2019), and previous studies on the pollution in this catchment (Martínez-Santos et al., 2015; García-García et al., 2019; Unda-Calvo et al., 2019) have highlighted the inputs of urban and (residual) industrial effluents treated through wastewater treatment plants (WWTP) located in the middle of the catchment, where phosphorus is eliminated using Cl_3Fe (only from May 1st to October 15th), resulting in the presence of metals in the water and sediment matrixes. The analysis of this anthropogenic influence has been monitored from April 2014 to January 2017 in 11 sampling locations in the main channel and tributaries, highlighting the nutrients and metal input of urban and industrial effluents. Furthermore, a recent study on this catchment has focused on the major ion chemistry of its waters, assessing the main geochemical processes input in relation to the anthropogenic input (Lechuga-Crespo et al., 2020b) while emphasising the influence of an evaporitic saline spring in the southwest part of the catchment, which exerts a great impact on the water chemistry downstream to the outlet of the catchment.

2.3.2 Set up of the QSWATLitho project

A local Digital Elevation Map (DEM, 25m resolution cell) was used to create the stream network, locate the outlet of the catchment, and delimit the drainage area. Subbasins were merged to obtain their draining to the sampling locations of the monitoring campaigns. A European land use map from the CORINE Land Cover project (100m resolution), a soil map from the Harmonized World Database (a 30 arc-second resolution), and

a local lithological map reclassified for the categories found in Hartmann and Moosdorf (2012) were combined with the DEM-derived slope map to create the HRUs (the description and source of the datasets may be seen in Table 1, Table 2, and Figure 3). While setting up the model, three slope ranges were established (0%-5%, 5%-10%, >10%) and no simplification was performed to reduce the number of HRUs. The weather input data was obtained from a hydrometeorological station located close to the outlet (Figure 3), consisting of precipitation as well as maximum and minimum temperature daily time series from January 1994 to December 2017. The observed data for discharge was covered from January 2004 to December 2017 for three gauging stations located close to the outlet and near the outlet of the two major subbasins of this catchment (see Figure 3). SWAT has been used to compute the hydrological representation of the case study, using the QSWATLitho HRU definition for the spatial discretization, but using the same water balance as the SWAT model.

Observed data for riverine chemical concentration ranged from April 2014 to January 2017. A monitoring program samples the river waters monthly or bimonthly using a pre-washed polypropylene bottle which was carried to the laboratory at 4ºC and filtered through 0.45µm filters. One replicate was acidified to 0.2% with HNO_3 (68%) for base cations (Ca^{2+}, Mg^{2+}, Na^{+}, and K^{+}) using ICP-OES (Perkin Elmer Optima 2000). The other non-acidified replicate was used to analyse anions (Cl^{-}, NO_3^{-}, SO_4^{2-}) through ion chromatography (DIONEX ICS 3000). Alkalinity was measured using a Total Organic Carbon Analyzer (TOC-L Shimadzu). The ionic charge balance (ICB) was within ±10% for all samples used in this study. For the modelling of the geochemical loads, groundwater and lateral flows from the SWAT hydrological representation have been used as a source of lithological chemical weathering derived loads, while runoff has been attributed to lower concentrations, inducing dilution in the stream's concentration.

Following the recommendations of ASABE (2017), three periods were defined in this project: a warmup period to reduce the effect of state variables' initial values (six years, January 1998-December 2003), a calibration period to optimise the parameters (ten years, January 2004-December 2013), and a validation period to test the model capabilities in an independent dataset (four years, January 2014-December 2017). The model's performance evaluation has been carried out for the calibration and validation periods independently, using graphical methods (time series between observed and simulated), and relative statistical measures (coefficient of determination, r^2, Nash-Sutcliffe Efficiency, NSE, PBIAS, and Kling-Gupta, KGE). The Moriasi et al. (2015) standard has been considered in this study to evaluate the model's performance. However, the authors have found no reference when comparing the daily loads of major ions, so the exploration of the results would yield the first reference for future similar analysis.

Table 1. Input data type, description and sources for the case study set up project used in the present study.

Input Data	Type	Description	Source
Digital Elevation Model (DEM)	Raster	A raster representing the elevations at 25x25m resolution	www.geoeuskadi.eus

Land Use	Raster	A raster representing the land uses of the catchment, at a resolution of 100x100m	https://land.copernicus.eu/pan-european/corine-land-cover
Soil Type	Raster	A raster representing the main types of catchment soil	http://webarchive.iiasa.ac.at/Research/LUC/External-World-soil-database/HTML/index.html?sb=1
Lithology	Raster	A derived raster representing the lithological classes of the catchment	www.geoeuskadi.eus
Precipitation and Temperature	Text File	Time series at one station with daily precipitation, maximum and minimum temperature	Spanish Agency of Meteorology (AEMET)

Table 2. Lithological distribution of the Deba River basin and its subbasins. Data derived from the Lithological Map of Euskadi (www.geoeuskadi.eus), reclassified for Hartmann and Moorsdorf's (2012) lithological categories. Original map and lithological classification are available in Supplementary Information (Figure S1 and Table S1).

	Main channel							Tributaries			
Lithology	**D1**	**D2**	**D3**	**D4**	**D5**	**D6**	**D7**	**M1**	**O1**	**E1**	**E2**
Area [km^2]	6.2	62.4	121.1	321.0	329.2	419.0	485.7	3.5	129.6	2.4	55.5
ev	4%	3%	7%	7%	7%	6%	7%		11%		
mt		25%	27%	11%	11%	9%	7%		3%		
pi							1%				
py				2%	2%	5%	5%				5%
sc	19%	11%	9%	16%	16%	15%	18%	3%	18%	2%	14%
sm	77%	54%	51%	60%	61%	61%	58%	97%	66%	98%	78%
ss		1%	1%	1%	1%						
su		6%	5%	3%	3%	2%	2%		3%		
vb				1%	1%	2%	3%				3%
wb									1%		

Lithological clases: evaporites (ev), metamorphics (mt), plutonic intermediate (pi), pyroclastics (py), carbonate sediments (sc), mixed sediments (sm), siliciclastic sediments (ss), unconsolidated sediments (su), volcanic basic (vb), water bodies (wb)

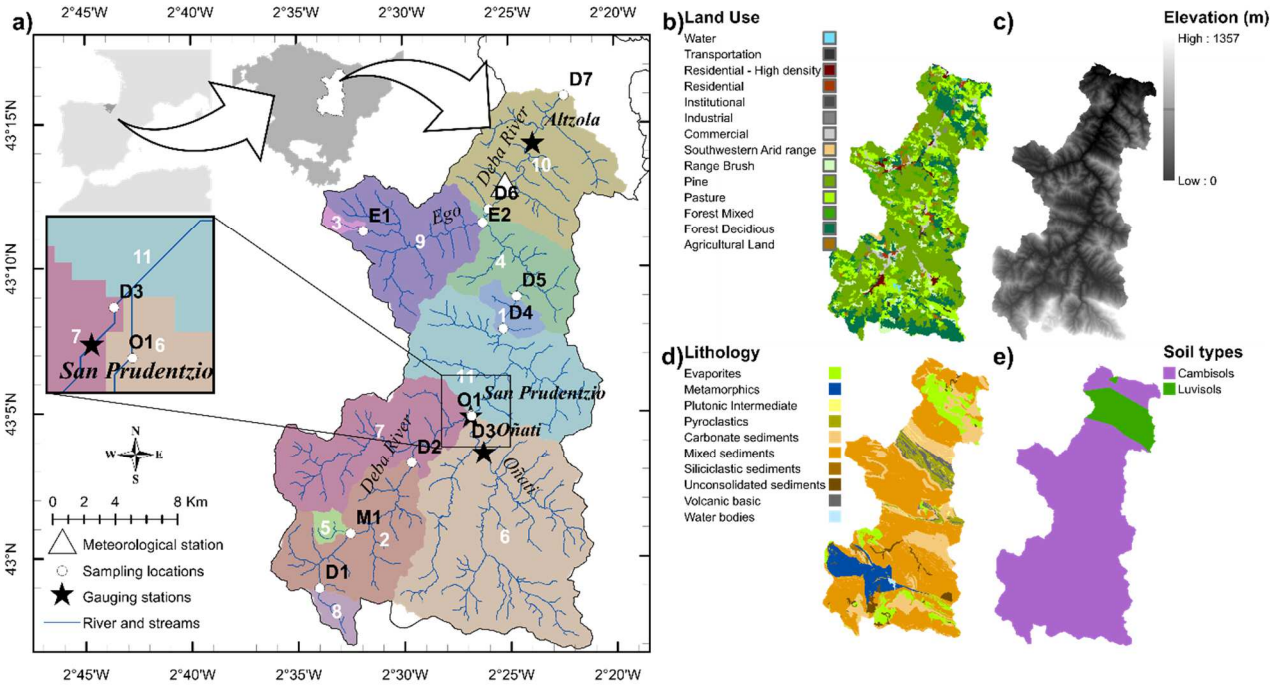

Figure 3. Deba River catchment description: a) localisation, main channel and tributaries, sampling locations, gauging stations and subbasins used in the present study; b) land use; c) digital elevation map; d) lithological units; e) soil types. Figures b), c), d), and e) are used for the setup of the model.

2.3.3 *Discharge parameterisation*

The geochemical reactions responsible for ionic loads derived from rocks to the river are assumed to be in equilibrium at daily scales; however, other sources like human input or atmospheric deposition are expected to vary in these temporal ranges. Thus, the simulation (both calibration and validation) has been done at a daily time step. The first step is to calibrate the discharge (in surface runoff, lateral flow, and groundwater flow), which will be the main drivers in the temporal application of the ICWR model. The discharge has been calibrated using the parameters found in Table 3, through both manual calibration and autocalibration with the SUFI-2 algorithm in SWAT-CUP (Abbaspour et al., 2007). Three gauging stations have been used to evaluate the model performance on discharge calibration using four statistical criteria: the coefficient of determination (r^2), the Nash & Sutcliff Efficiency (NSE), the percent of bias (PBIAS), and the Kling-Gupta efficiency (KGE). All the statistics are applied to the simulated and observed values: r^2 focuses in the fit between the trends, varying from 0 (no fit) to 1 (perfect fit); PBIAS calculates the global over- (negative value) or underestimation (positive value); NSE evaluates the trends (similar to r^2, but varying from -∞ to 1, perfect fit); and KGE is based on Pearson's coefficient "r", including bias and variability, ranging from -∞ to 1 (perfect fit), where values > -0.41 could be considered as a reasonable performance (Knoben et al. 2019).

Table 3. Parameters modified for calibration, type of change (v: value change, r: relative change), description and change adopted.

File	Change type	Parameter name	Description	Best fit	Minimum	Maximum
gw	v	GW_DELAY	Groundwater delay time	240.5	200	500
	v	ALPHA_BF	Baseflow alpha factor	0.27	0.05	0.3
	v	GWQMN	Threshold depth of water in shallow aquifer required for return flow to occur	1081	600	1500
hru	v	LAT_TTIME	Lateral flow travel time	3.31	1	7
	r	HRU_SLP	Average HRU slope	↓15%	↓30%	0
	v	CANMX	Maximum canopy storage	17.8	5	20
mgt	r	CN2	Curve number for moisture condition II	↓26%	↓30%	0
sol	r	SOL_AWC	Available water capacity	↓11%	↓20%	↑30%
	r	SOL_K	Soil hydraulic conductivity	↑5%	-	↑30%

2.3.4 *Downscaling the ICWR model*

The original ICWR model (Lechuga-Crespo et al., 2020a) was developed for an annual average specific flux output for which only the average specific discharge was needed for hydrology. To explore the possibilities of applying this model at lower spatial and temporal scales, three assessments have been performed: a model's sensitivity analysis, a spatial evaluation, and a temporal assessment. The model's sensitivity to input data was evaluated by testing different global and local datasets combinations. Two lithological maps, one clipped from the Global Lithological Map (GLiM, Hartmann and Moosdorf, 2012), and a local one obtained from the Gipuzkoa Council (geoeuskadi.eus), together with two annual average specific discharges, one obtained from a global dataset (UNH/GRD, Fekete et al., 2002) and other from the Gipuzkoa Council Hydrological Department (www.gipuzkoa.eus), were combined to obtain four output datasets. The comparison with observed data indicated the best input data setup for building the QSWATLitho project. These results are

shown and discussed in section *3.1.1 Model's sensitivity to input data*. Before applying the SWATLitho module, it is necessary to calibrate the water balance. The model setup and the calibration of hydrology are discussed in section *3.1.2 Case study*. Once the model was built and hydrology was calibrated, a simulation was conducted (period: January 2014 to December 2017). The application of the SWATLitho module allowed the evaluation of the model's spatial and temporal performance. No calibration of the ICWR parameters has been done, and globally fitted values were used (Lechuga-Crespo et al., 2020a). The model's spatial downscaling evaluation was done by contrasting simulated geochemical loadings at the subbasin outlet with observed loadings at the corresponding sampling location (see Figure 3a). Results are presented in section *3.1.3 Spatial downscaling*. The temporal downscale was evaluated at three gauging stations, where daily loadings were derived from punctual data and continuous registries integration. The results are shown in section *3.1.4. Temporal downscaling*. Finally, model limitations, improvement suggestions, and alternatives are presented in section *3.1.5 SWATLitho limitations and alternatives*. Even though the wide applicability of the model makes this approach versatile, its setup may be constrained by input data availability.

A proposed alternative approach is the use of digital filters to deconvolute the hydrological signal between surface and groundwater fluxes. In this sense, we computed the hydrological deconvolution using the Eckhardt digital filter (Eckhardt 2005; Xie et al., 2020). This test has been performed at the three gauging stations of the catchment.

3 Results and discussion

3.1.1 Model's sensitivity to input data

Average annual loadings obtained for the four input data combinations are shown in Table 4. The original ICWR model (Lechuga-Crespo et al., 2020a) was calibrated and validated using global data (method UNH+GLIM in Table 4) and data on rivers worldwide from the GLORICH database. The highest values among all methods considered are found for the UNH+GLIM method, and the greatest differences are found not between the two hydrological datasets but between the lithological maps. This confirms that the lithological representation has a major impact on the loadings computed by the model. Regarding the values obtained with the four datasets in comparison with the observed values (Gauging station in Table 4), the closest values are found for the EUS+GEUS method, the local data for hydrology and lithology. Nevertheless, the difference between the observed and the modelled values are different between ions and gauging stations. Both the Altzola and San Prudentzio gauging stations present the highest differences in Ca^{2+}, Na^{+}, K^{+} and Cl^{-}, while the differences between the observed and the simulated values are lower for other ions. Such differences are not found in the Oñati tributary, where the highest difference is found for Mg^{2+}, Cl^{-}, and SO_4^{2-}, but which is still lower than the Altzola and the San Prudentzio bias for the previously noted ions. The common pattern in the differences found for Altzola and San Prudentzio and the difference for the Oñati stream suggest that

311 there is a common phenomenon not captured by the model's performance in the San Prudentzio draining
312 basin, which affects downstream at the outlet of the catchment.

313 The monitoring program and previous studies in the area (Iribar and Ábalos 2011; Martínez-Santos et al.,
314 2015) have shown that the southeastern part of the catchment has the highest values of Ca^{2+}, Na^{+}, K^{+}, and Cl^{-},
315 which is related to the presence of gypsum intrusions and a spring, altering the local water's composition. In
316 both lithological maps used, the intrusion of gypsum (evaporites) in the southwest part of the catchment seems
317 to be underestimated. In addition, according to Iribar and Ábalos (2011), the southern part of the catchment
318 contains a combination of different geological registries (Albian and Aptian-Albian) where there is a common
319 presence of springs with saline waters. Within this catchment, the Leintz-Gatzaga spring contains one of the
320 most concentrated effluents to the streams (230.6 $g \cdot L^{-1}$ according to Iribar and Ábalos, 2011). This suggests
321 that the impact of the saline is not properly mapped in either the global or the local lithological maps, but that
322 it exerts a strong influence on the chemical characteristics of this area downstream (Lechuga-Crespo et al.,
323 2020b). For this reason, the observed data on Na^{+}, K^{+}, and Cl^{-} are higher than those modelled, especially in the
324 San Prudentzio subbasin. The inclusion of a local lithological map, with a finer spatial resolution of lithology,
325 has decreased the loads to around half of those obtained with the previous map. These new values are closer to
326 reality when considering Mg^{2+}, HCO_3^{-}, and SO_4^{2-}, which are the elements less affected by the spring inputs.
327 The inclusion of a spatially distributed lithology has improved the results of the model, leading to the
328 conclusion that increasing the spatial resolution of the lithology input data has a major effect on the output of
329 the model.
330 From the model's sensitivity analysis, we conclude that when applying the ICWR model to local studies, local
331 lithological data should be applied. Moreover, consideration of saline springs should be taken into account
332 when evaluating the model's performance.

333 **Table 4**. The table demonstrates the average annual loadings that were obtained using the ICWR model in the Deba River catchment,
334 with different input data. UNH represents the global hydrological dataset (UNH/GRDC, Fekete et al., 2002), the EUS indicates the
335 local average data from the Gipuzkoa Council Hydrological Department (www.gipuzkoa.eus), the GLIM denotes the global
336 lithological map (GLIM, Hartmann and Moosdorf, 2012), the GEUS implies the local lithological map (www.geoeuskadi.eus),
337 Gauging station represents the data obtained from each gauging station. All values expressed as mean annual load in [$Mg \cdot y^{-1}$].

Method	Ca^{2+}	Mg^{2+}	Na^{+}	K^{+}	Cl^{-}	HCO_3^{-}	SO_4^{2-}
Altzola							
UNH+GLIM	24783	5923	3707	755	6675	104465	20457
EUS+GLIM	22393	5352	3349	682	6031	94389	18484
UNH+GEUS	10492	2262	1991	348	3272	45897	14792
EUS+GEUS	9480	2044	1799	314	2957	41470	13365
Gauging station	20777	1755	6358	1050	10485	55244	14513
Oñati							
UNH+GLIM	6918	1651	1019	210	1842	28922	5640
EUS+GLIM	7233	1726	1066	220	1926	30238	5897
UNH+GEUS	2852	589	525	78	881	12565	4152
EUS+GEUS	2981	616	549	82	921	13137	4341

Gauging station	3894	294	314	84	381	10918	1861
San Prudentzio							
UNH+GLIM	5353	1287	861	164	1513	23340	4646
EUS+GLIM	4237	1019	681	130	1198	18473	3677
UNH+GEUS	2034	416	384	70	642	8871	2971
EUS+GEUS	1610	330	304	56	508	7021	2351
Gauging station	5691	497	2526	394	4266	14865	4381

3.1.2 Case study set-up and discharge calibration

The combination of slope, land use, soil types, and lithological classes in this catchment leads to a spatial discretisation consisting of 11 subbasins and 985 HRUs. When building the same project considering land use, soil type, and slope layers in the HRU definition step, the number of spatial units reaches 286 HRUs. A more detailed project regarding spatial distribution increases the computation time, but the water balance calibration is more comprehensive, which is a key input for the geochemical loads' computation, and the model's temporal downscaling.

Regarding the calibration of hydrology at the daily time step (Figure 4), most of the parameterisation has been focused on calibrating groundwater and lateral flow, which account for almost 96% of the annual discharge at the catchment's outlet. The parameterisation of the model has yielded the results summarised in Table 5, and Moriasi et al. (2015) qualifies the simulation as "Satisfactory" for calibration and validation. According to these results, the model has been considered enough to represent the hydrology of the catchment studied.

NSE is used based on its performance, which is better when the variable's range of variation is large. However, in low flows, the denominator tends towards 0, leading to higher values when the errors are small (Oeurng et al., 2011). The higher values for r^2 in comparison to the NSE suggest a good representation of the dynamic, but a worse depiction of the exact discharge value, indicating a difference between observed and simulated values which is stronger in lower flow periods. This can also be seen in the PBIAS, where the calibration for San Prudentzio has yielded a value classified as "Non-Satisfactory" according to Moriasi et al. (2015). A negative value of the PBIAS proposes an underestimation of the model, which is attributed to peaks in the drier period of the simulation. Fluctuations are related to the way groundwater is calculated in SWAT, not using a spatially diffused flow, but pulses in each HRU (Bailey et al., 2019). Improvements in the model performance for hydrology may be expected by incorporating a more detailed soil map, as the present resolution seems too coarse for the needs of this modelling.

The most sensible parameters are the SCS curve number (CN2.mgt), which was decreased to adjust the peak discharge in combination with the maximum canopy storage (CANMX.hru), the baseflow recession constant (ALPHA_BF.gw) and the lateral flow travel time (LAT_TTIME.hru).The lateral flow has a relevant role in the hydrology of this catchment. Baseflow was adjusted using the delay of water passing through the last soil

366 layer (GWDELAY.gw) and the water threshold in the shallow aquifer needed for groundwater flow to occur
367 (GWQMIN.gw). All specific changes are shown in Table 3.

368

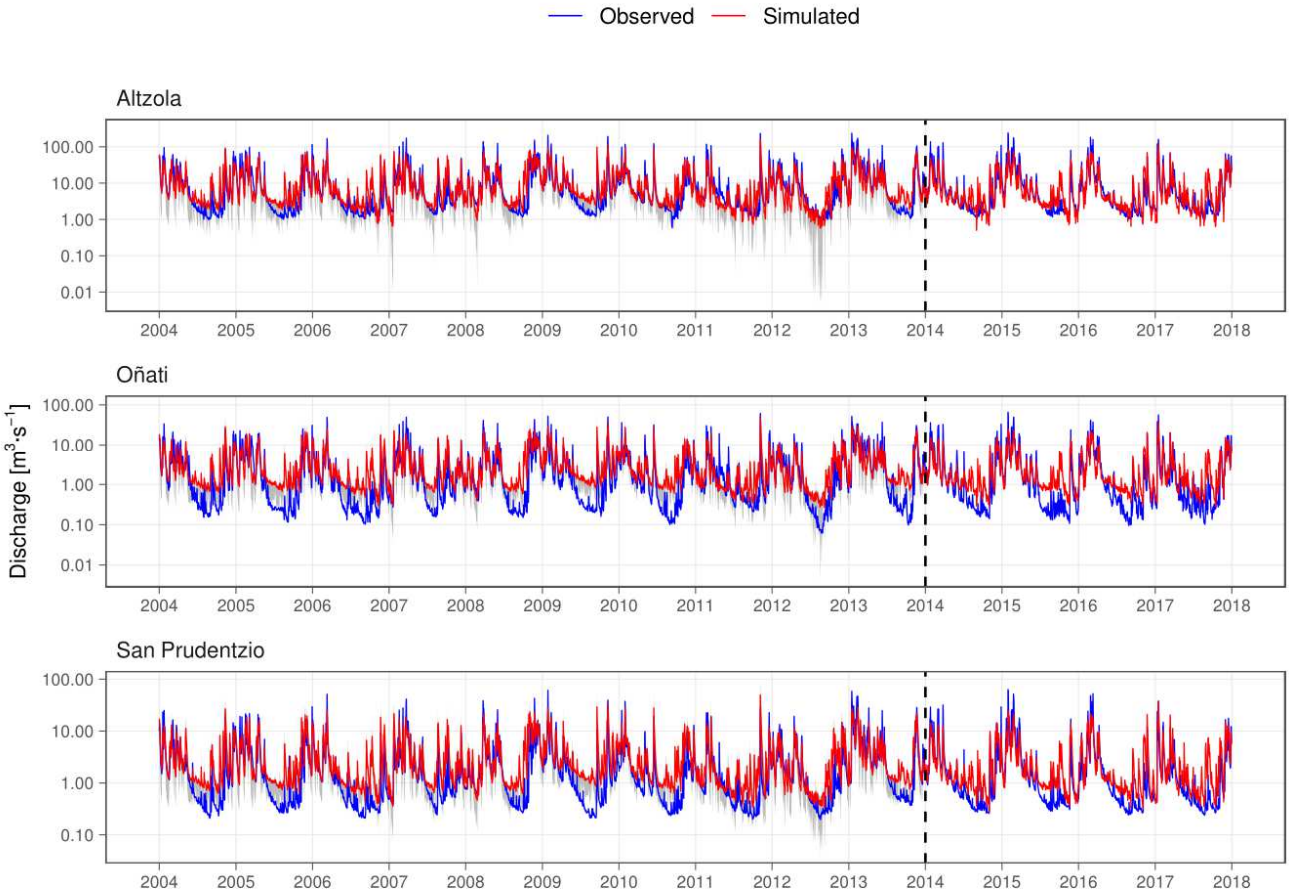

369

370 **Figure 4.** Time series of daily simulation and observation discharge in three sampling locations in the catchment. A dashed line
371 separates the calibration from the validation period. The grey band in the calibration period represents the 95th lower and upper limits
372 of the 100 simulations performed using the SUFI2 algorithm in SWATCUP (Abbaspour et al., 2007, 2014). As there is a relevant
373 difference in discharge ranges between the dry and the wet periods, the vertical axis is plotted in logarithmic scale.

374 **Table 5.** Summary of hydrological calibration and validation in three gauging stations at a daily time step. r^2 represents the coefficient
375 of determination, where 0 = no correlation and 1 = perfect fit; NSE is the Nash-Sutcliffe Efficiency, where < 0 = observed mean better
376 than simulation, 0 = model prediction is accurate as observed mean, and 1 = perfect fit; PBIAS represents the tendency of the
377 simulation to be larger or smaller than the observations, where >0 = overestimation of the model, <0 = underestimation of the model,
378 KGE is the Kling-Gupta Efficiency, where values >-0.41 are considered as reasonable (Kobne et al., 2019), and 1 = perfect fit. *P-*
379 *factor* represents the fraction of the measured data falling within the 95% prediction uncertainty band, while *r-factor* is the ratio of the
380 average width of the band and the standard deviation of the measured variable.

	Calibration						**Validation**			
	January 2004 - December 2013						**January 2014 - December 2017**			
	r^2	**NSE**	**PBIAS (%)**	**KGE**	**p-factor**	**r-factor**	**r^2**	**NSE**	**PBIAS (%)**	**KGE**
Altzola	0.72	0.71	-0.7	0.71	0.65	0.42	0.76	0.68	13.7	0.56
Oñati	0.64	0.64	-13.5	0.71	0.47	0.48	0.74	0.71	0.9	0.64
San Prudentzio	0.65	0.62	-28.4	0.64	0.57	0.5	0.7	0.66	-4.8	0.60

3.1.3 Spatial downscaling

The geochemical loadings derived from rock's chemical weathering are carried out by the rivers to oceans and lakes. Disregarding instream transformation (outgassing, biological uptake, secondary precipitation, or ionic exchange processes) loadings are added along the river network. Figure 5 presents the comparison of these loadings at the outlet of each subbasin, which has a corresponding sampling location. Only fluxes from sampling campaigns are considered (cf. Lechuga-Crespo et al., 2020b). As expected, there is a corresponding generally increasing trend between the two signals. Downstream sampling locations have higher exports than upstream subbasins. However, the trend is different for each ion.

Mg^{2+}, SO_4^{2-}, and HCO_3^- present the best spatial collinearity among all ions, and the mean loadings in each sampling location are scattered around the perfect fit line. The largest deviations are Na^+ and Cl^-, where observed values are higher than the simulation ones. Nevertheless, since loadings are added through the routing network, upstream errors are carried downstream. Specific attention to the D2 and D3 sampling locations (subbasins 2 and 7, respectively) indicate underestimation for all ions, especially Na^+ and Cl^-. This suggests that this area contains an ionic point source loaded with these ions, which is not captured by the model. This results in the worst representation among all of the catchments.

Among the headwater sampling locations (D1, E1, M1, and O1) and subbasins (8, 3, 5, and 6, respectively), the Oñati stream presents the largest loadings, in which ions are commonly located close to the perfect fit line except for Mg^{2+} and SO_4^{2-}. This overestimation compensates for the underestimation found in D3 for these ions, improving the overall representation of the model. Further analysis of this stream's temporal evolution is found in section *3.1.4 Temporal downscaling*.

The application of the model to this case study supports that headwater locations present lower discrepancies than downstream subbasins. This spatial analysis indicates that point sources exert a great impact on the model's performance, since downstream locations are conditioned by incoming loadings.

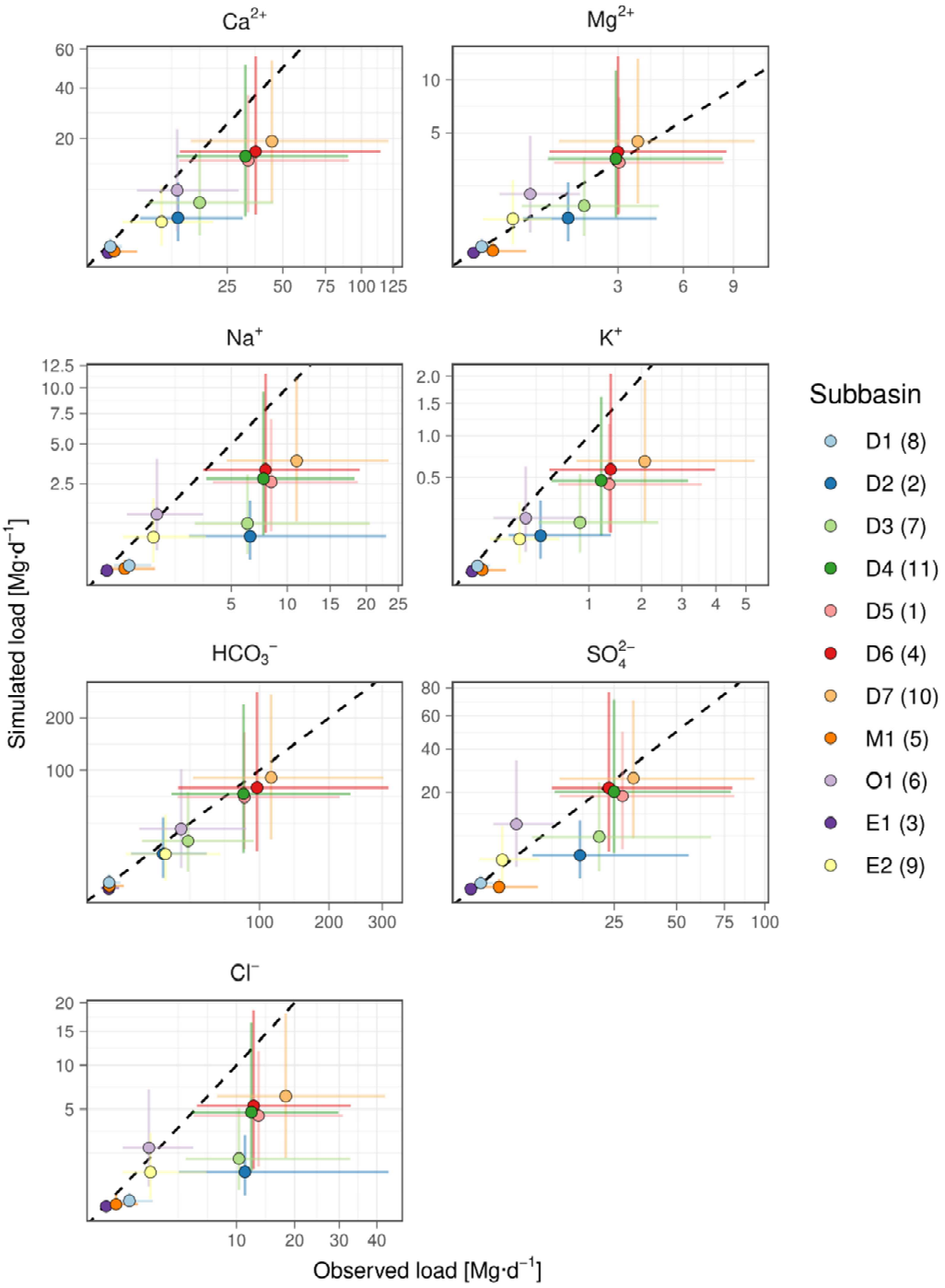

406

407 **Figure 5.** Simulated versus observed loadings for all sampling locations (subbasin number presented between
408 brackets). The point represents the mean value for the daily loadings, considering only dates with *in-situ*
409 monitoring campaigns. Horizontal and vertical lines present minimum and maximum values for observed and
410 simulated loadings.

411 *3.1.4 Temporal downscaling*

412 Figure 5 presents a graphical assessment of the SWATLitho performance, comparing the simulated and
413 observed time series at three gauging stations (Altzola, San Prudentzio, and Oñati, Figure 3a). A visual

evaluation shows that the global fitted parameters applied to the calibrated QSWATLitho project yield geochemical loads showing a varying degree of similarity between the simulated and the observed values, suggesting the model performs differently depending on the ion and drainage basin being considered. Besides, Table 6 contains the statistical results for each pair of time series and the average values for each gauging station. Considering Altzola results as representative of the catchment-scale performance of the model, the average statistics show a reasonable performance from the model (r^2 = 0.74 ± 0.02, PBIAS=-17.96 ± 85.02, KGE=0.08 ± 0.48), according to the criterion presented by Kobne et al. (2019) regarding KGE.

Focusing on the subbasin-scale, each mean statistic yields a different pattern for the model's performance. The mean coefficient of determination (r^2) is comparable among gauging stations, suggesting that dynamic representation is homogeneous at the subbasin level. The mean percentage of deviation (PBIAS) indicates that the Altzola gauging station is the closest to reality, while Oñati presents the largest discrepancies; the Kling-Gupta Efficiency factor (KGE), as a summary statistic, is best for San Prudentzio and worst for Oñati. However, the analysis of the standard deviation highlights the presence of two outliers in Oñati: Mg^{2+} and SO_4^{2-}. Excluding these outliers from the analysis yields the best values for Oñati in all statistics (KGE = 0.59 ± 0.19, PBIAS[%] = 13.22 ± 34.68, and r^2 = 0.75 ± 0.01), and worst for San Prudentzio. The Altzola gauging station, which receives waters from Oñati, San Prudentzio and other tributaries in the main channel, presents intermediate statistics suggesting that the differences present in the upper part of the catchment are routed downstream to the outlet. This can also be seen in the times series in Figure 5, where the deviations between the observed and the simulated values are similar in Altzola and San Prudentzio, while they are independent at the Oñati stream. Using the KGE as an integrative measure of the model's performance, values >-0.41 are considered reasonable (Kobne et al., 2019). This criterion yields a valid representation of the average ionic loadings in all gauging stations.

Previous studies in the area using *in-situ* samplings have highlighted the sulphate water composition in the Oñati stream of the catchment (Lechuga-Crespo et al., 2020b), which could be related to the evaporitic presence in the upper part of the catchment (Iribar and Ábalos, 2011). However, despite the evaporitic presence in the input data (largest percentage the in draining catchment, Table 2), a karstic presence has also been reported in the area (Iribar and Ábalos, 2011), which could be a source of diluted water to the system. A complex interaction of these saline and diluted water sources may be responsible for the discrepancies found between the simulated and the observed values for Mg^{2+} and SO_4^{2-}.

In addition, the presence of springs, i.e. wells with saline water, is common in the San Prudentzio stream (Iribar and Ábalos, 2011), particularly the Leintz-Gatzaga spring, which provides one of the most concentrated effluents, with 230.6 $g \cdot L^{-1}$ of total dissolved solids and over 85 $g \cdot L^{-1}$ of Cl^- (Iribar and Ábalos, 2011). The vertical pathway of this spring is over 384 m (Iribar and Ábalos, 2011), which explains the different dynamics of Cl^-, Na^+, and K^+ present in this area, as the input from the spring is steadier than the

448 rapid response of the groundwater and the lateral flow of the remaining catchment, changing the relative
449 contribution of these ions to the total cation concentration with time (Lechuga-Crespo et al., 2020b).

450 There are few models similar to this one, but a recent publication (Bailey et al., 2019) introduced a saline
451 module based on physical equations at chemical equilibrium into the SWAT code to analyse of the fate and
452 transport of the ions in catchments. In addition, the researchers in that study reported problems of
453 underestimation of the model's value regarding unmapped mineral presence in the input data, which also
454 occurred in the present study. Both studies have shown the importance of measured concentrations in rivers as
455 a proxy for the geochemical minerals affecting the riverine loads. In the present case, the monitoring
456 campaigns, together with the gauging station's data, have recorded the effect of the spring input, which the
457 model did not capture.

458

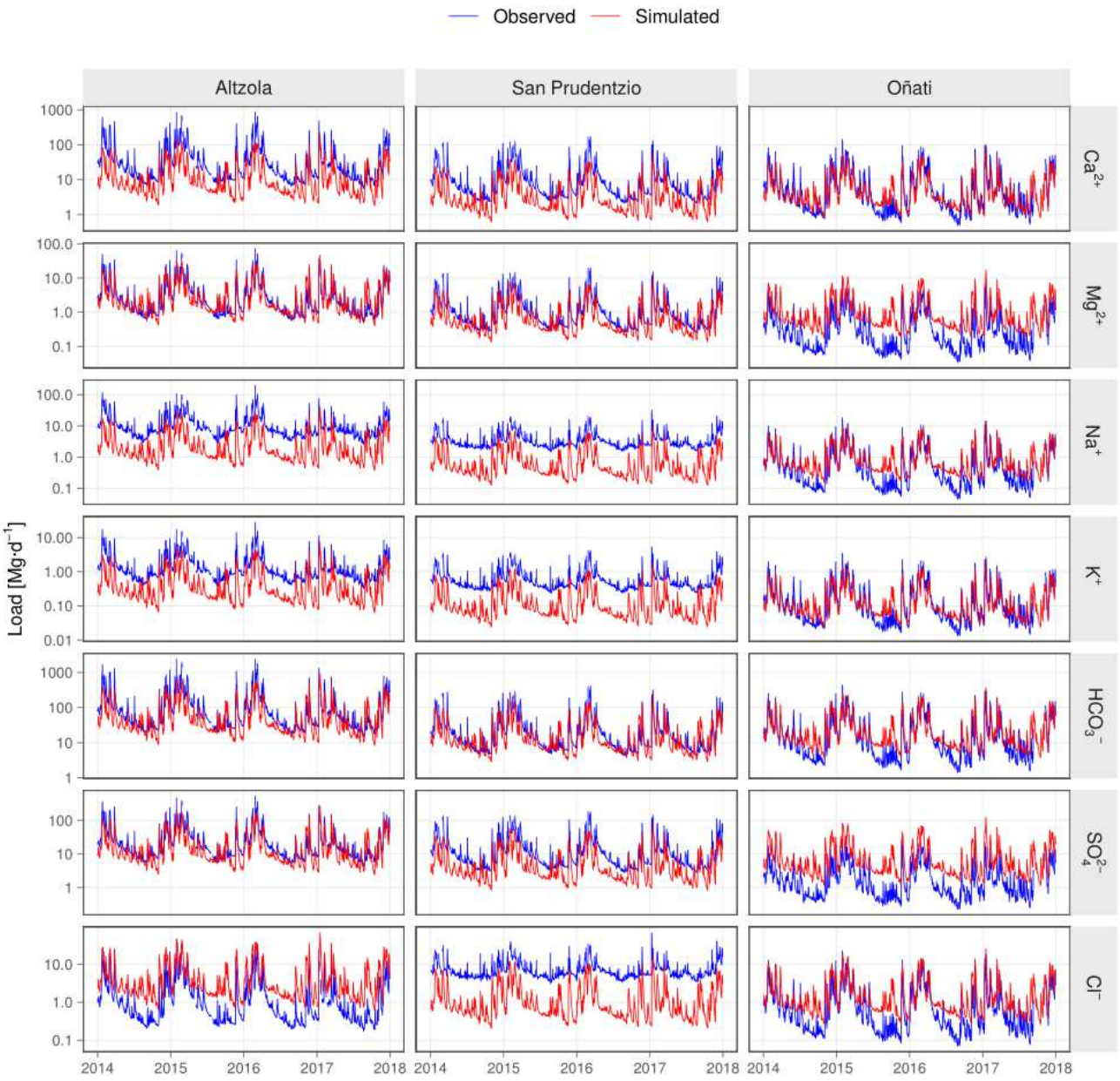

Figure 6. Time series (validation period: January 2014-December 2017) of daily simulated and observed loadings at three gauging stations, Altzola, San Prudentzio, and Oñati, of Ca^{2+}, Mg^{2+}, Na^{+}, K^{+}, SO_4^{2-}, Cl^{-}, and HCO_3^{-}. The gauging stations are located in the outlet of the catchment and in two tributaries. Note that the vertical axis is in logarithmic scale to better differentiate the results in dry and wet periods.

Table 6. Summary statistics for geochemical loadings in the Deba River urban catchment. The coefficient of determination is represented by r^2, where 0 = no correlation, and 1 = perfect fit. NSE is the Nash-Sutcliffe Efficiency, where <0 = observed mean better than simulation, 0 = model prediction is accurate as observed mean, and 1 = perfect fit. PBIAS denotes the tendency of the simulation to be larger or smaller than the observations, where >0 = overestimation of the model, and <0 = underestimation of the model. KGE is the Kling-Gupta Efficiency, where values >-0.41 are considered as reasonable (Kobne et al., 2019), and 1 = perfect fit. *mean* and *sd* signify the arithmetic mean and standard deviation of all ions for each gauging station.

Station	Ion	r^2	PBIAS [%]	KGE
Altzola	Ca^{2+}	0.76	-67.70	-0.02
	Mg^{2+}	0.76	-9.80	0.68
	Na^{+}	0.70	-73.90	-0.04
	K^{+}	0.72	-66.60	0.05
	HCO_3^{-}	0.75	-44.30	0.26

	SO_4^{2-}	0.76	-31.10	0.46
	Cl^-	0.73	167.70	-0.84
	mean	0.74	-17.96	0.08
	sd	0.02	85.02	0.48
San Prudentzio	Ca^{2+}	0.75	-64.40	0.04
	Mg^{2+}	0.75	-38.40	0.38
	Na^+	0.70	-76.90	0.00
	K^+	0.73	-76.20	-0.02
	HCO_3^-	0.74	-28.30	0.47
	SO_4^{2-}	0.76	-58.10	0.15
	Cl^-	0.65	-80.50	-0.04
	mean	0.73	-60.40	0.14
	sd	0.04	20.26	0.21
Oñati	Ca^{2+}	0.74	-23.00	0.55
	Mg^{2+}	0.75	169.20	-1.10
	Na^+	0.75	25.40	0.70
	K^+	0.75	-13.80	0.64
	HCO_3^-	0.75	13.10	0.79
	SO_4^{2-}	0.67	284.30	-2.90
	Cl^-	0.75	64.40	0.29
	mean	0.74	74.23	-0.15
	sd	0.03	112.97	1.38

3.1.5 SWATLitho limitations and alternatives

A recent study has presented a physically-based module for assessing the fate and transport of saline ions in catchments integrated on the SWAT model (Bailey et al., 2019). That model has been developed to evaluate the best irrigation management practices and their impacts on the salinisation of freshwater environments within a catchment. The setup requirements are a discharge calibrated SWAT project, the initial concentrations of the ions in the soil and the aquifer, and the percentage of five solid species present in each HRU to compute the chemical equilibrium (Bailey et al., 2019). In contrast, the model introduced in the present study focuses solely onthe process of chemical weathering. It computes the geochemical loadings derived from lithology to the river streams based on empirical equations; uses a lithological and soil description, as well as hydrology, as its input data. The SWATLitho model is not based on a spatial mineralogical representation but on lithological groups of minerals that are available worldwide (cf. Hartmann and Moosdorf, 2012) or commonly available in finer resolution for local studies. However, it lacks point source data (for irrigation, saline springs, or other anthropogenic inputs). In fact, even though the SWAT model has been widely applied (Fu et al., 2019), there may be occasions when it is not possible to set up the model even though there is interest exists in assessing the chemical weathering derived geochemical loadings in a dynamic way.

Applying the SWATLitho model to evaluate daily loadings at a local scale has yielded reasonable results for representing the dynamic ($r^2 > 0.73$). However, applying the model to local-scale studies to quantify daily draining loads at the catchment's outlet is conditioned by a detailed representation of the area's lithology and the lack of other relevant salt sources. When considering the Altzola gauging station as a reference for the

catchment-scale model application, the mean percentage of deviation of the model is ~-17.96% (Table 6). The results shown here do not include any variation in the mineral dissolution constant (c_{xi} in Equation 1) which is likely to occur with changes in groundwater or lateral flow water temperature. A more mechanistic model is needed to account for this evolution, as well as the chemical equilibrium between phases (as done in Bailey et al., 2019). However, the more mechanistic a model is, the harder it is to find available input data.

In the present study, a digital filter to deconvolute the hydrograph –distinguish surface runoff from baseflow and lateral flow with the total discharge time series– has been tested as a potential alternative when it is not possible to set up QSWATLitho projects, either because of a lack of input data or computational resources constraints. Interannual daily loads (mean, first, and third quartiles) are shown monthly in Figure 7. Spatial and temporal limitations of the SWATLitho model have been discussed in previous sections (3.1.3 and 3.1.4), but all three results in the Oñati drainage catchment, observed, SWATLitho and Eckhardt, present a similar temporal pattern. However, the SWATLitho presents a peak for all ions in September. This is not present in the other two methods, supporting the idea that the SWAT's groundwater flux computation is affected by pulses calculated in each HRU instead of a diffuse load, which is better represented by graphical separation in an Eckhardt model. Nonetheless, the variances of the two methods have yielded discrete values, though a Welch's test for the differences between the loadings SWATLitho and the Eckhardt module has yield a $p>0.05$, which does not demonstrate enough significance to indicate that the loadings are dissimilar. The visual inspection and the test demonstrate that the Eckhardt digital filter may be applied when a QSWATLitho project cannot be set up.

One of the limitations of the ICWR model is the presence of spring waters or point sources that alter the streams' composition. Those impacts are not presented in the model at this stage and should be considered when assessing the chemical loads from catchments with springs within their hydrogeological basin or groundwater inputs that are sourced outside the hydromorphological basin. When it comes to the model's performance from various input data, the greatest distinctions among results in the loadings have been found when changing the lithological map, yielding results closer to the observed values.

Future improvements of the SWATLitho model should allow the inclusion of saline point sources (which could represent natural saline springs or anthropogenic inputs), and permit the calibration of the c_{xi} parameters for each catchment (which could adjust the contribution of each lithology for each location) as done in the common SWAT calibration procedure.

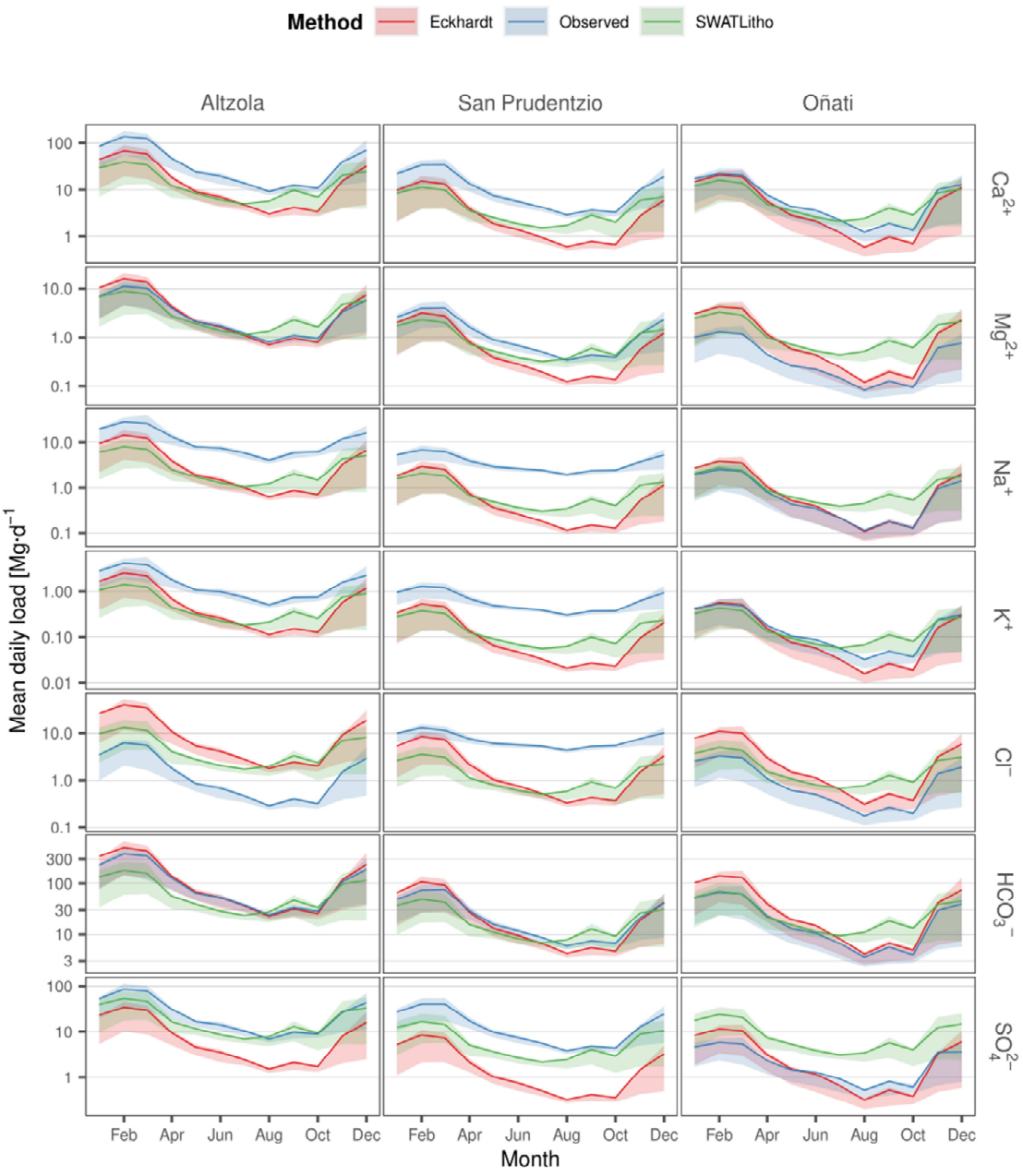

Figure 7. Average monthly inter-annual loading comparison among the observed, SWATLitho, and Eckhardt digital filter results. Lines indicate the mean value, while the shade represents the 1st and 3rd quartiles for the January 2014 to December 2017 time series. The vertical axis is shown in logarithmic scale.

4 Conclusion

An empirical model used to estimate the annual average geochemical loads to rivers through chemical weathering has been downscaled from global to local scale, and shifted from an annual average estimation to a daily dynamic output, based on the coupling with SWAT, an extended hydrological model. The coupling method is described along with the case study, using different input datasets to check the influence of hydrology and lithology resolution in the outputs of the model. The use of globally fitted parameters for the model has yielded average loadings with a model underestimation of 17.96% with regards to the observed

data, though the model's performance is "reasonable" on the representation of spatially explicit daily geochemical loadings to stream the a catchment level.

The limitations of the model have been addressed, such as the poor performance of the model when springs are present in the study area, or when the lithological input dataset does not contain information hydrogeochemically relevant units, such as gypsum intrusions, which are too small to be mapped but relevant enough to affect the water chemistry and loadings. An alternative has also been presented for those cases in which a QSWATLitho project cannot be set up: the application of a digital filter to measure data in a gauging station, together with the drainage basin description (lithology and soil classes). The results do not present significant differences from those of the SWATLitho, which suggests that both methods may be applied when it is not possible to set the first one up or that spatially explicit results are not in the scope of the modelling.

The present work introduces a hydrogeochemical tool which is useful for estimating dynamic chemical weathering loadings out of a catchment at a local scale and also for the estimating of ionic fluxes that derive from the chemical weathering of rocks in a spatiotemporal context.

Software availability

- The Soil and Water Assessment Tool (SWAT) is freely available in https://swat.tamu.edu/software/
- The QGIS plugin for SWAT (QSWAT) is freely available in https://swat.tamu.edu/software/qswat/
- The modified QGIS plugin that is presented in this study (QSWATLitho) as well as the SWATLitho module written in Python are freely available in https://swat.tamu.edu/software/swat-litho/

Acknowledgements

The authors wish to thank the Consolidated Group "Hydro-Environmental Processes" (IT 1029-16, Basque Government), the University of the Basque Country (UPV/EHU) (UFI 11/26), and the Institut National Polytechnique de Toulouse (INPT) for supporting this project. The authors declare no conflict of interest. Author contributions: J.L.L.C. helped with the conceptualisation, methodology, software, validation, formal analysis, data curation, investigation, writing (original draft, review and editing), and in visualization; S.S. worked on the conceptualisation, methodology, validation, writing (review and editing), resources, investigation, supervision, and project administration; E.R.R. collaborated during the investigation, validation, resources, data curation, supervision, and funding acquisition; C.G. assisted with during the methodology, software, validation, resources, and writing (review and editing); J.M.S.P. supported during conceptualisation, methodology, software, validation, investigation, resources, writing (review and editing), supervision, and project administration.

References

Abbaspour, K. C., Vejdani, M., Haghighat, S., & Yang, J. (2007). SWAT-CUP calibration and uncertainty programs for SWAT. *In MODSIM 2007 International congress on modelling and simulation, modelling and simulation society of Australia and New Zealand* (pp. 1596-1602).

Allison, J. D., Brown, D. S., & Novo-Gradac, K. J. (1991). *MINTEQA2/PRODEFA2, A geochemical assessment model for environmental systems: version 3.0 user's manual*. Athens, Georgia 30613: United States Environmental Protection Agency.

American Society of Agricultural and Biological Engineers (ASABE). (2017). *Guidelines for Calibrating, Validating, and Evaluating Hydrologic and Water Quality (H/WQ) Models.*

Amiotte-Suchet, P., & Probst, J. L. (1995). A global model for present-day atmospheric/soil CO2 consumption by chemical erosion of continental rocks (GEM-CO2), *47B*, 273–280. https://doi.org/10.1034/j.1600-0889.47.issue1.23.x

Arnold, J. G., Moriasi, D. N., Gassman, P. W., Abbaspour, K. C., White, M. J., Srinivasan, R., . . . Jha, M. K. (2012). SWAT: Model use, calibration, and validation. *Transactions of the ASABE*, *55*(4), 1491–1508. https://doi.org/10.13031/2013.42256

Arnold, J. G., Srinivasan, R., Muttiah, R. S., & Williams, J. R. (1998). Large area hydrologic modeling and assessment: Part I: Model development. *Journal of the American Water Resources Association*, *34*(1), 73–89. https://doi.org/10.13031/2013.42256

Bailey, R. T., Tavakoli-Kivi, S., & Wei, X. (2019). A salinity module for SWAT to simulate salt ion fate and transport at the watershed scale. *Hydrology and Earth System Sciences*, *23*(7), 3155–3174. https://doi.org/10.5194/hess-23-3155-2019

Cañedo-Argüelles, M., Kefford, B., & Schäfer, R. (2018). Salt in freshwaters: Causes, effects and prospects - introduction to the theme issue. *Philosophical Transactions of the Royal Society of London. Series B, Biological Sciences*, *374*(1764). https://doi.org/10.1098/rstb.2018.0002

Dile, Y. T., Daggupati, P., George, C., Srinivasan, R., & Arnold, J. (2016). Introducing a new open source GIS user interface for the SWAT model. *Environmental Modelling & Software, 85*, 129–138. https://doi.org/10.1016/j.envsoft.2016.08.004

Dürr, H. H., Meybeck, M., & Dürr, S. H. (2005). Lithologic composition of the Earth's continental surfaces derived from a new digital map emphasizing riverine material transfer. *Global Biogeochemical Cycles*, *19*(4), n/a-n/a. https://doi.org/10.1029/2005GB002515

Eckhardt, K. (2005). How to construct recursive digital filters for baseflow separation. *Hydrological Processes, 19*(2), 507–515. https://doi.org/10.1002/hyp.5675

Fekete, B. M., Vörösmarty, C. J., & Grabs, W. (2002). High-resolution fields of global runoff combining observed river discharge and simulated water balances. *Global Biogeochemical Cycles*, *16*(3), 1-10. https://doi.org/10.1029/1999GB001254

Fu, B., Merritt, W. S., Croke, B. F., Weber, T. R., & Jakeman, A. J. (2019). A review of catchment-scale water quality and erosion models and a synthesis of future prospects. *Environmental Modelling & Software*, *114*, 75–97. https://doi.org/10.1016/j.envsoft.2018.12.008

García-García, J., Ruiz-Romera, E., Martínez-Santos, M., & Antigüedad, I. (2019). Temporal variability of metallic properties during flood events in the Deba River urban catchment (Basque Country, Northern

Spain) after the introduction of sewage treatment systems. *Environmental Earth Sciences*, *78*(1), 402. https://doi.org/10.1007/s12665-018-8014-1

Gipuzkoa Council. Cuenca del Deba. Retrieved from https://www.gipuzkoa.eus/es/web/obrahidraulikoak/hidrologia-y-calidad/informacion-general/nuestras-cuencas/deba

Goddéris, Y., François, L. M., Probst, A., Schott, J., Moncoulon, D., Labat, D., & Viville, D. (2006). Modelling weathering processes at the catchment scale: The WITCH numerical model. *Geochimica et Cosmochimica Acta*, *70*(5), 1128–1147. https://doi.org/10.1016/j.gca.2005.11.018

Hartmann, J., & Moosdorf, N. (2012). The new global lithological map database GLiM: A representation of rock properties at the Earth surface. *Geochemistry, Geophysics, Geosystems*, *13*(12), 119. https://doi.org/10.1029/2012GC004370

Hartmann, J., Moosdorf, N., Lauerwald, R., Hinderer, M., & West, A. J. (2014). Global chemical weathering and associated P-release — The role of lithology, temperature and soil properties. *Chemical Geology*, *363*, 145–163. https://doi.org/10.1016/j.chemgeo.2013.10.025

Iribar, V., & Ábalos, B. (2011). The geochemical and isotopic record of evaporite recycling in spas and salterns of the Basque Cantabrian basin, Spain. *Applied Geochemistry*, *26*, 1315–1329. https://doi.org/10.1016/j.apgeochem.2011.05.005

Kaushal, S. S., Duan, S., Doody, T. R., Haq, S., Smith, R. M., Newcomer Johnson, T. A., . . . Stack, W. P. (2017). Human-accelerated weathering increases salinization, major ions, and alkalinization in fresh water across land use. *Applied Geochemistry : Journal of the International Association of Geochemistry and Cosmochemistry*, *83*, 121–135. https://doi.org/10.1016/j.apgeochem.2017.02.006

Knoben, W. J. M., Freer, J. E., & Woods, R. A. (2019). Technical note: Inherent benchmark or not? Comparing Nash–Sutcliffe and Kling–Gupta efficiency scores. *Hydrology and Earth System Sciences*, 23(10), 4323–4331. https://doi.org/10.5194/hess-23-4323-2019

Lechuga-Crespo, J. L., Sánchez-Pérez, J. M., Sauvage, S., Hartmann, J., Amiotte Suchet, P., Probst, J. L., & Ruiz-Romera, E. (2020a). A model for evaluating continental chemical weathering from riverine transports of dissolved major elements at a global scale. *Global and Planetary Change, 192*, 103226. https://doi.org/10.1016/j.gloplacha.2020.103226

Lechuga-Crespo, J. L., Ruiz-Romera, E., Probst, J.-L., Unda-Calvo, J., Cuervo-Fuentes, Z. C., & Sánchez-Pérez, J. M. (2020b). Combining punctual and high frequency data for the spatiotemporal assessment of main geochemical processes and dissolved exports in an urban river catchment. *The Science of the Total Environment, 727*, 138644. https://doi.org/10.1016/j.scitotenv.2020.138644

Martínez-Santos, M., Probst, A., García-García, J., & Ruiz-Romera, E. (2015). Influence of anthropogenic inputs and a high-magnitude flood event on metal contamination pattern in surface bottom sediments from the Deba River urban catchment. *The Science of the Total Environment*, *514*, 10–25. https://doi.org/10.1016/j.scitotenv.2015.01.078

Meybeck, M., & Helmer, R. (1989). The quality of rivers: from pristine stage to global pollution. *Palaeogeography, Palaeoclimatology, Palaeoecology*, *75*, 283–309. https://doi.org/10.1016/0031-0182(89)90191-0

M'Nassri, S., Lucas, Y., Schäfer, G., Dridi, L., & Majdoub, R. (2019). Coupled hydrogeochemical modelling using KIRMAT to assess water-rock interaction in a saline aquifer in central-eastern Tunisia. *Applied Geochemistry*, *102*, 229–242. https://doi.org/10.1016/j.apgeochem.2019.01.018

Moriasi, D. N., Gitau, M. W., Pai, N., & Daggupati, P. (2015). Hydrologic and Water Quality Models: Performance Measures and Evaluation Criteria. *Transactions of the ASABE*, *58*(6), 1763–1785. https://doi.org/10.13031/trans.58.10715

Neitsch, S. L., Arnold, J. G., Kiniry, J. R., & Williams, J. R. (2011). *Soil and Water Assessment Tool: Theoretical Documentation Version 2009*: Texas Water Resources Institute Technical Report No. 406.

Oeurng, C., Sauvage, S., & Sánchez-Pérez, J. M. (2011). Assessment of hydrology, sediment and particulate organic carbon yield in a large agricultural catchment using the SWAT model. *Journal of Hydrology*, *401*(3-4), 145–153. https://doi.org/10.1016/j.jhydrol.2011.02.017

Parkhurst, D. L., & Appelo, C. A. J. (2013). *Description of Input and Examples for PHREEQC Version 3—A Computer Program for Speciation, Batch-Reaction, One-Dimensional Transport, and Inverse Geochemical Calculations. Chapter A43. Techniques and Methods: Vol. 6*. Denver, CO 80225: United States Department of the Interior. Retrieved from http://pubs.usgs.gov/tm/06/a43/

Schoups, G., Hopmans, J. W., Tanji, K. K. (2006). Evaluation of Model Complexity and Input Uncertainty of Field-Scale Water Flow and Salt Transport. *Vadose Zone*, *5*, 951–962. https://doi.org/10.2136/vzj2005.0130

Unda-Calvo, J., Ruiz-Romera, E., Fdez-Ortiz de Vallejuelo, S., Martínez-Santos, M., & Gredilla, A. (2019). Evaluating the role of particle size on urban environmental geochemistry of metals in surface sediments. *The Science of the Total Environment*, *646*, 121–133. https://doi.org/10.1016/j.scitotenv.2018.07.172

Xie, J., Liu, X., Wang, K., Yang, T., Liang, K., & Liu, C. (2020). Evaluation of typical methods for baseflow separation in the contiguous United States. *Journal of Hydrology, 583*, 124628. https://doi.org/10.1016/j.jhydrol.2020.124628